WCTE 2016
World Conference on Timber Engineering
August 22-25, 2016 | Vienna, Austria

INFLUENCE OF AN AFRP RETROFIT SOLUTION WHEN APPLIED TO TIMBER FRAMED MASONRY PANELS

Andreea Dutu, Hiroyasu Sakata, Yoshihiro Yamazaki, Tomoki Shindo

ABSTRACT:

Although the timber framed masonry (TFM) structures are usually an earthquake resistant traditional architecture, for some of them the construction details are poor. Connections are the weakest parts of the system, especially the bottom ones, at every floor level or at the connection with foundation, and if not executed properly, the entire safety of the structure may be in danger. To solve this problem, a retrofit solution was investigated and uni-directional AFRP sheets were applied on full scale timber framed masonry wall parts (one module and four modules) and in-plane static cyclic tests were conducted. The test results showed the efficiency of the retrofit solution. The paper presents a discussion on the contribution in strength and ductility of one diagonal AFRP sheet, and also the influence of the main parameters (thickness of the aramid sheet and corresponding bonding area).

KEYWORDS: retrofit, timber, masonry, AFRP

1 INTRODUCTION

Although the timber framed masonry (TFM) structures are considered earthquake resistant, for many of them the construction details are poor. Connections are weakest parts of the system, especially the bottom ones, at every floor level or at the connection with foundation. Also, in past earthquakes out-of-plane collapse was observed usually for the upper masonry panels, though without causing a general collapse of the building [1].
Since for some countries the system can be found in heritage buildings, a retrofitting solution was studied in order to improve the behavior of timber framed masonry structures.
The experimental tests were conducted in Japan, where masonry structures are quite scarce, thus workmanship and materials are not easy to find, therefore the specimen's construction details were chosen based on the Portuguese timber framed masonry heritage buildings type (Pombaline), as a continuation of previous studies [2], but without the timber diagonals (St. Andrew's cross). The structure without the diagonals can be found in other countries' timber framed masonry buildings, like Romania, Nepal, or China.
The connections were cross-halving type that is common for many of the TFM structures (Portuguese, Italian, Haitian, etc.) [3; 4; 5].
The experiments described in this paper were the second phase of a project that studied the mechanical behavior when subjected to lateral force for TFM [5].
AFRP sheets (uni-directional) were applied on two types of TFM specimens (1 module and 4 modules), and the results of static cyclic tests under in-plane loading are further observed and discussed.

2 EXPERIMENTAL TESTS

Four specimens were tested and compared, at two different levels. First, one panel specimens (one module) were tested, with and without retrofit, and afterwards, four panel specimens (four modules) were tested in static cyclic loading (Fig. 1).
The parameters that were studied were the thickness of the AFRP sheet, the corresponding bonding area, and the influence of the retrofit solution on the ductility and damage pattern. In the same time, the contribution of one aramid sheet to the strength of the specimen was observed.

[1] Andreea Dutu, Technical University of Civil Engineering Bucharest, andreea.dutu@utcb.ro
[2] Hiroyasu Sakata, Tokyo Institute of Technology, Japan, sakata.h.aa@m.titech.ac.jp
[3] Yoshihiro Yamazaki, Tokyo Institute of Technology, Japan, yamazaki.y.ai@m.titech.ac.jp
[4] Tomoki Shindo, Tokyo Institute of Technology, Japan shindo26648@gmail.com

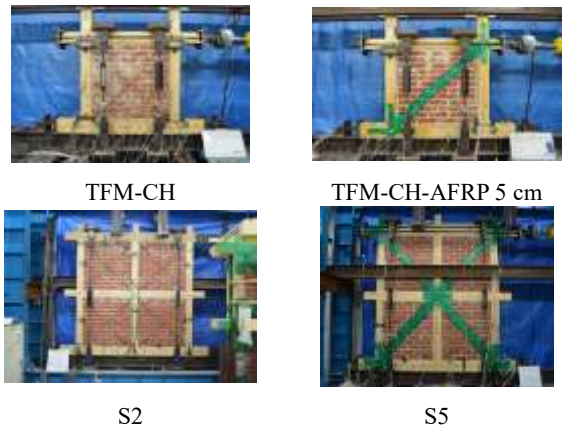

Figure 1: *Experimental study on timber framed masonry (TFM-CH and S2), timber framed masonry retrofitted with uni-directional sheet (TFM-CH-AFRP and S5), at two scales of TFM panels (1 module and 4 modules)*

The wall specimens had the same dimensions for the tests with and without retrofit, as shown in Figure 2 and Figure 3.

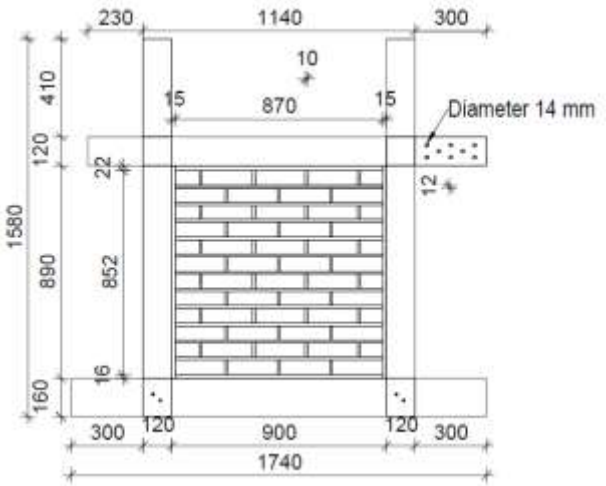

Figure 2: *Not-retrofitted specimen TFM-CH (one module)*

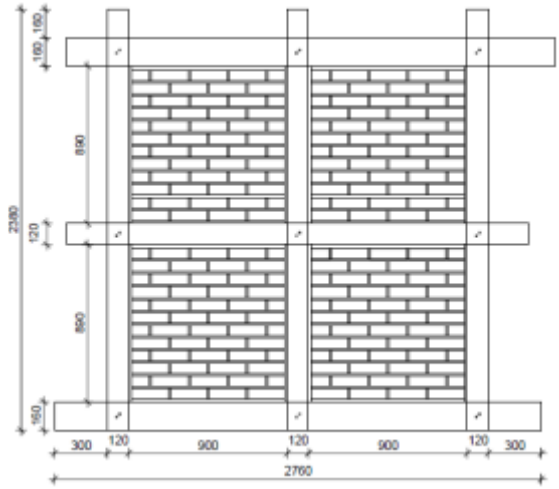

Figure 3: *Not-retrofitted specimen S2 (four modules)*

The size of the panels was according to the real scale of a Pombaline structural wall (Portuguese type of TFM structure), but instead of having 3 masonry panels per height, the present experimental study's specimens' was erected with only 2 panels per height due to space limitation of the testing facility. The tests were carried out on a reaction frame having an actuator with a capacity of 200 kN and a jack's stroke of 500 mm. A vertical force was initially introduced through pretension steel tie rods and uniformly distributed on the top of the specimen using steel plates connected to the upper beam with screw nails. This value was calculated as the equivalent force acting on a first floor wall in a four story tall building. The vertical force was uniformly distributed on the top of the wall specimen using steel plates connected to the upper beam with screw nails. Out of plane deformation was restrained using four jigs with rollers to avoid friction at the top of the wall for S2 and with two steel beams on which teflon sheet was applied to reduce friction (TFM-CH, TFM-CH-AFRP 5 cm, S5), respectively. Setup is shown in Fig. 4.

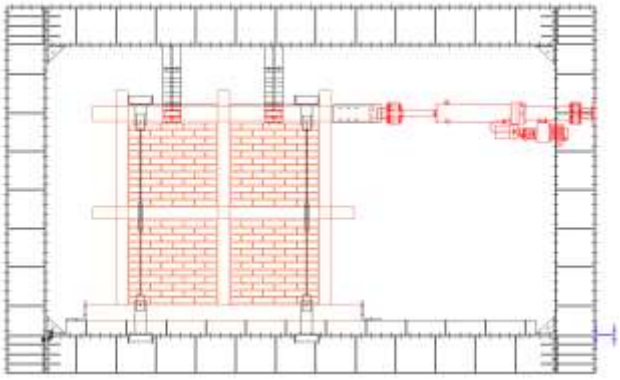

Figure 4: *Test setup scheme [6]*

The CUREE – Caltech standard protocol for wood frames was used with a loading history consisting of initiation cycles, primary cycles and trailing cycles (Figure 6).

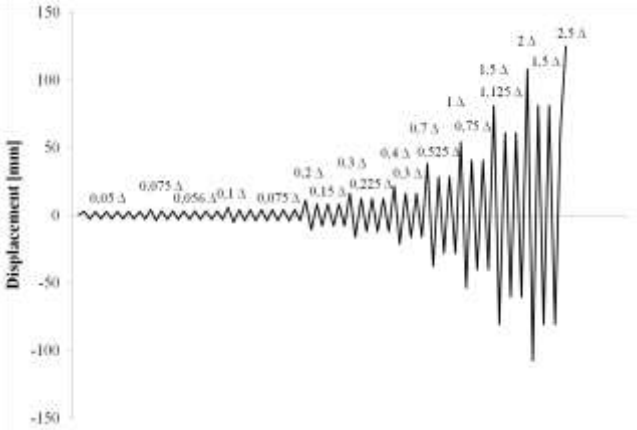

Figure 5: *Loading protocol [6]*

The aramid fiber sheets used were uni-directional. The tensile capacity provided by producer was 90 tf/m, the Young's modulus was 118 kN/mm^2 and the thickness of the sheet was 0.430 mm. Application procedure is shown in Fig. 6.

The sheets were attached by means of epoxy resin, after previous application of a primer and epoxy glue which helped to uniform the surface of the masonry and also

areas at the corners of the infills and the timber frame's connections.

Figure 6: *Application of the AFRP sheet on S3 and S4, respectively [7]*

The width of all the sheets for TFM-CH-AFRP was 5 cm and the lengths differ as shown in Fig. 7, while for S5 the width of the sheets was 10 cm. Fig. 8 shows the dimensions and layout of the AFRP sheets applied on the specimen S5.

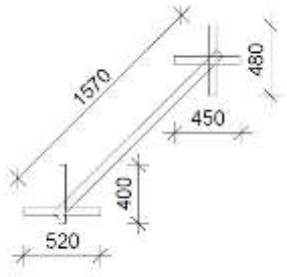

Figure 7: *Dimensions and layout of the AFRP sheets – TFM- [7]*

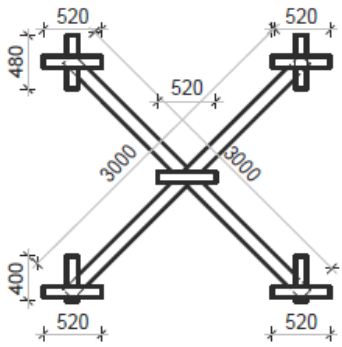

Figure 8: *Dimensions and layout of the AFRP sheets – S5 [7]*

The strain in the AFRP sheets was measured by means of strain gauges, uni-directional, bi-directional and three-directional type positioned as shown in Fig. 9 and Fig. 10, respectively.

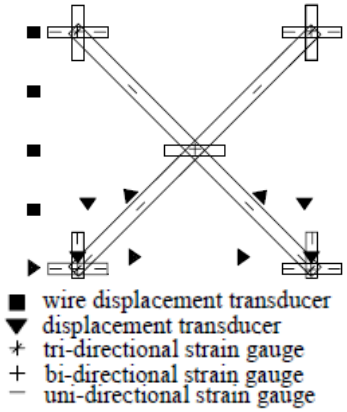

Figure 9: *Layout of the measurement devices [7]- S5*

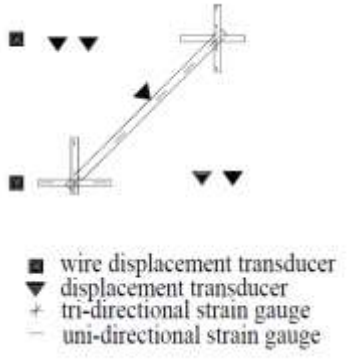

Figure 10: *Layout of the measurement devices [7]- S5*

3 TEST RESULTS

One module specimens

The comparison at the one panel level (Fig. 11) in terms of force – share angle shows that the aramid sheet is contributing only to the strength increase of the specimen until aramid breaks. The retrofit experiment was stopped at 0.05 radians, while the non-retrofitted one was continued until 0.08 radians.

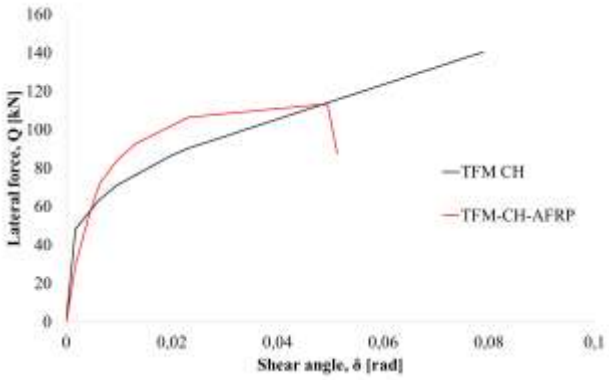

Figure 11: *Comparison of envelope curves between TFM-CH and TFM-CH-AFRP*

The AFRP strips failed due to the cracks caused by compression in reverse cycles along the diagonal of the masonry panel.

Figure 12: *Fracture of the AFRP sheet on the front side of the bottom connection (TFM-CH-AFRP)*

Figure 13: *Fracture of the AFRP sheet on the back side of the bottom connection (TFM-CH-AFRP)*

The damages during the tests indicate that not all the sheets are loaded. The diagonal, the vertical on front bottom connection and the horizontal on the back bottom connection are showing cracks or exploded during the last cycles.
The masonry panel separated from the timber frame from early cycles. The cracks in the masonry are similar for both specimens.

Four module specimens

For the four panels' level, a high ductility increase can be observed (Fig. 14). The retrofitted specimen deformed until 0.06 radians without a major decrease in strength. At this value of the drift, the stroke of the jack had finished, for the available setup. The maximum strength was around 150 kN. The damages first appeared in the masonry panels, both bottom and upper ones, and around 0.03 radians, the AFRP strips started to fracture. After the failure of the AFRP strips, the system continued to work at an average strength of 130 kN until the stop of the experiment.

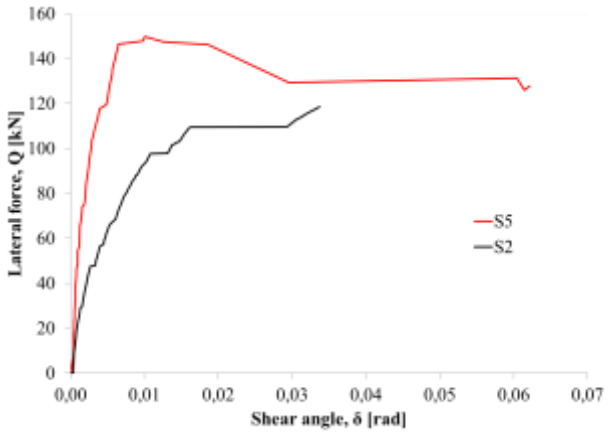

Figure 14: *Comparison of envelope curves between S2 and S5*

The AFRP strips failed in a different way, depending on the side of the specimen that they are applied on. On the front side, the vertical and diagonal sheets were subjected to tensile force, due to the uplift tendency (Fig. 15, 16 and 17).

Figure 15: *Damages of the AFRP sheets on the front side (S5)*

Figure 16: *Fracture of the AFRP sheet on the front side of the bottom right connection (S5)*

Figure 17: *Fracture of the AFRP sheet on the front side of the bottom left connection (S5)*

On the backside (Fig. 18), the horizontal sheets were mostly subjected to shear force. The general tendency was that the sheets detached first from the masonry panels, due to the irregularity of the surface, so the strength of the wall depended mainly on the bonding strength between the AFRP sheet and the timber element.

Figure 18: *Fracture of the AFRP sheet on the back side of the bottom right connection (S5)*

The sheets on the masonry panels contributed more to the stiffness of the wall, considering the fact that after these detached, the stiffness started to decrease until the fracture, when the behavior was based on the timber and masonry assemble alone, without the contribution of the sheet.

4 BONDING STRENGTH AFRP-MASONRY

Material tests were conducted in order to identify the bonding strength between the AFRP and the masonry, considered an important parameter in the behavior of the retrofitted walls and in the effectiveness of the fiber. Masonry prisms on which AFRP sheets were attached were tested by pull-off of the sheet. The specimen layout and testing scheme are shown in Fig. 19.

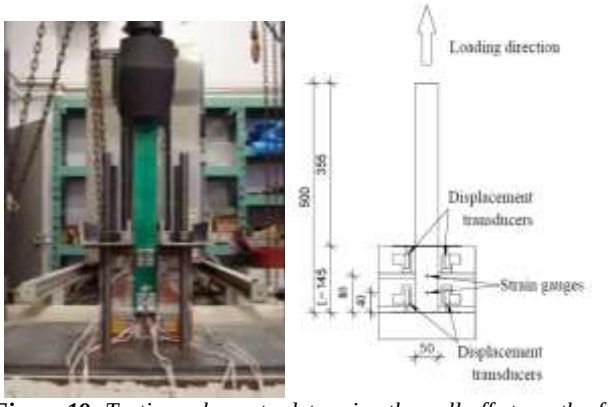

Figure 19: *Testing scheme to determine the pull off strength of AFRP-masonry prism assemble*

The tensile stress applied to the AFRP, being the force recorded by the testing machine, that caused failure of the strengthening is showed in Table 1.

Table 1: *Test results for pull-off test AFRP-masonry*

Specimen	Tensile stress [N/mm^2]	Bonding strength at the loading end [N/mm^2]
1	408,8	1,21
2	483,8	1,43
3	570,1	1,69
4	553,0	1,64
5	623,1	1,85
Average	**527,8**	**1,57**
CoV	**15,7%**	

The debonding occurs mainly by detaching the sheet with thin layers of brick and mortar on it. However, as it can be recognized in Fig. 19, on some areas, mostly next to the loaded end of the sheet, there is no brick or mortar layer detached. This failure mode does not influence the tensile strength of the AFRP that produces the debonding.

Figure 20: *Failure modes of all tested specimens*

Bonding stress distribution is obtained by analytical approach proposed by Oliveira et al, 2011 [8] that considers equation 1 based on the differentiation of the bonding strength, τ, obtained by equilibrium of the system:

$$\tau(x_i) = \frac{1}{2} E_{FRP} t_{FRP} \cdot \cdot \left[\frac{\varepsilon_{FRP}(x_i) - \varepsilon_{FRP}(x_{i-1})}{x_i - x_{i-1}} + \frac{\varepsilon_{FRP}(x_{i+1}) - \varepsilon_{FRP}(x_i)}{x_{i+1} - x_i} \right] \quad (1)$$

Where E_{FRP} is the Young's modulus of the aramid fiber, given by producer as 118 GPa, t_{FRP} is the thickness of the AFRP

sheet, ε_{FRP} is the strain value obtained by strain gauges and x_i is the length from the unloaded end to the strain gauge position. Fig. 21 shows the bonding stress distribution along the bonded length for 50% and 100% of the maximum recorded load.

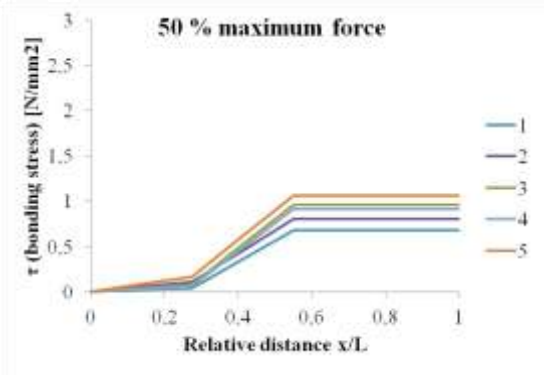

Figure 21: *Bonding stress distribution vs. relative distance for each masonry prism tested (50% maximum force)*

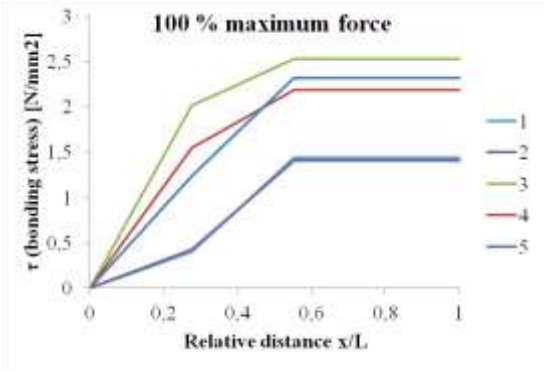

Figure 22: *Bonding stress distribution vs. relative distance for each masonry prism tested (100% maximum force)*

The average bonding strength between the AFRP and masonry resulted in 1,56 N/mm^2, thus almost two times more than the one obtained by Tezuka et al., 2004 [9] for the bonding between AFRP and timber, 0.875 N/mm^2, for an epoxy resin type provided by the same manufacturer.

5 STRESS DISTRIBUTION ON AFRP SHEETS (S5)

Considering the result above, the stress recorded by strain gauges were compared for the sheets applied on both TFM-CH-AFRP and S5, only for the timber connections. The positions of the strain gauges are shown in Fig. 9. The stress values are shown for 4 levels of displacement at the top of the wall, as percentage of the maximum value recorded.

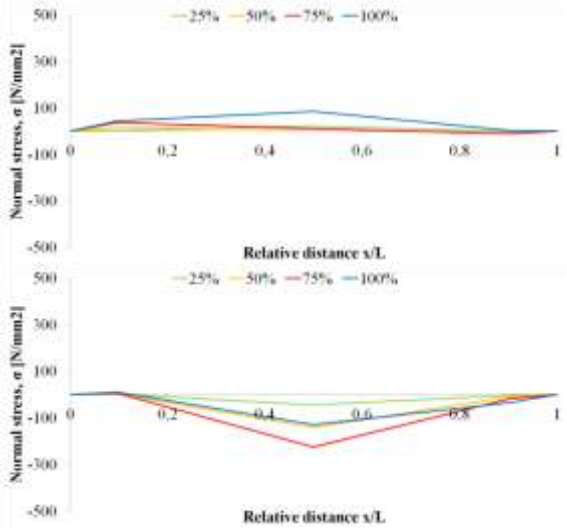

Figure 23: *Normal stress distribution on horizontal AFRP sheets applied on the bottom connections (back side) - S5*

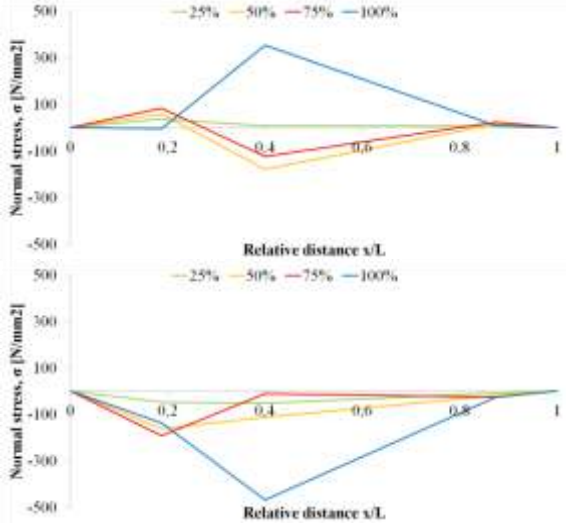

Figure 24: *Normal stress distribution on vertical sheets applied on the left (up) and right (down) bottom connections (front side) - S5*

6 STRESS DISTRIBUTION ON AFRP SHEETS (TFM-CH-AFRP)

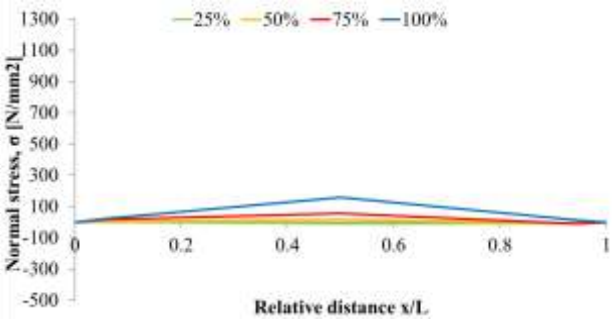

Figure 25: *Normal stress distribution on horizontal sheets applied on the bottom connections (back side) - TFM-CH-AFRP*

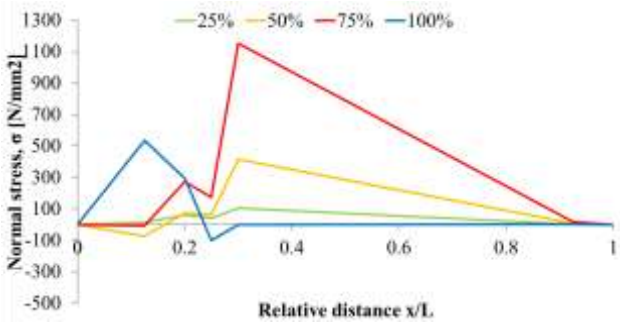

Figure 26: *Normal stress distribution on vertical sheets applied on the bottom connections (front side) - TFM-CH-AFRP*

7 DISCUSSION

The test results are confirming in both cases an increase in strength of the specimens, with an approximate value of 7 kN for the 5 cm width aramid sheet (one piece) and 20 kN for the 10 cm width aramid sheet (one piece).
Table 2 shows the values of the lateral force at 0.02 radians shear angle and corresponding increase given by the aramid sheet.

Table 2: *Lateral force at 0.02 radians shear angle*

Specimen	AFRP strip width [cm]	Lateral force [kN]	Difference in lateral force divided by the number of strips [kN]
TFM-CH	-	85.92	6.99
TFM-CH-AFRP	5	99.91	
S2	-	103.11	20.43
S5	10	143.96	

The damage pattern comparison between specimens with and without retrofit for both test specimen levels, one module and four modules (Fig. 27 and 28), shows a more uniform distribution of the cracking in the masonry infill panels, which indicates better energy dissipation in the infill for both retrofitted cases.

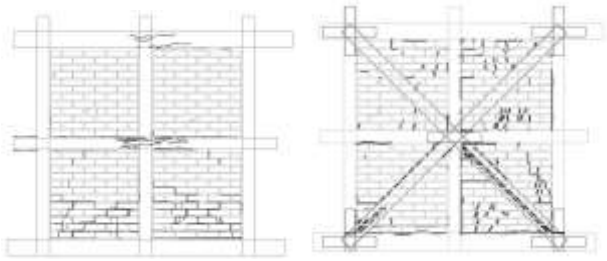

Figure 27: *Comparison of crack pattern between S2 and S5*

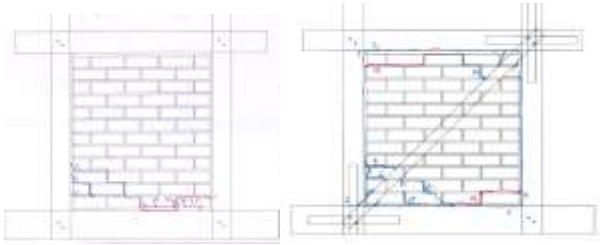

Figure 28: *Comparison of crack pattern between TFM-CH and TFM-CH-AFRP*

Knowing the bonding strength between timber and AFRP [10] and assuming the effective bonding area on the timber connections [8], the force necessary for debonding is obtained. This force divided by the thickness and width of the sheet gives the maximum expected normal stress in the sheet, summarized in Table 3.

Table 3: *Normal stress evaluation in the sheets, depending on the effective bonding area*

Specimen (side)	Bonding strength (timber-AFRP) [N/mm^2]	Assumed effective bonding area [mm^2]	Dimensions of the sheet, width x thickness [mm]	Expected normal stress [N/mm^2]
S5 (front side)	0.875	28306	100 x 0.43	575
S5 (back side)		42577		866
TFM-CH-AFRP (front side)		14370	50 x 0.43	585
TFM-CH-AFRP (back side)		32980		1342

When compared with the recorded values from the strain gauges for S5 (Figure 23-24) and for TFM-CH-AFRP (Figure 25-26), it can be seen that for the vertical sheets on the bottom connections on the front side of the specimens, the maximum values recorded are closer to the expected normal stress. In the same time, for the back side it is not the same situation, the values being much lower than the one expected. This situation can also be confirmed by the damages, which are more on the front side.
This confirms the difference in behavior for front side and back side of the specimens, for both one module and four modules. For this conclusion, the layout of the cross-halved connection also contributes, due to the difference between its front and back side.
Additionally, this implies that prediction of the behavior of the sheets is particularly difficult due to this reason and the evaluation of the aramid sheet contribution should focus more on the parts of the connection which exhibit uplift in the non-retrofitted state, i.e. on front side the vertical sheet.

8 CONCLUSIONS

S5 and TFM-CH-AFRP tests indicated that one diagonal AFRP sheet can increase the overall strength, by its tensile deformation, with approximately 20 kN and 7 kN, respectively. The vertical sheets work on the front side bottom connections mainly, while on the back side the horizontal ones, but the contribution of the latter ones is not so significant.

The cyclic behavior of the test has a major contribution in the damage pattern, as it was observed that in compression the AFRP sheet cracks and then fractures.

The use of fiber reinforced polymers is known to be highly dependent on the workmanship and when used for masonry, the capacity prediction evaluation process is characterized with even more uncertainty due to the non-homogenous and inelastic behavior of it. The above described tests show that each fiber behaves differently, depending on the quantity of used resin, or the smoothness of the surface. This also may influence the general stability of the wall.

The retrofit solution was effective in terms of strength and damage pattern. The AFRP does not increase the stiffness of the specimen, and this is an advantage since the TFM system shows, by nature, a high ductility. This property is recommended to be maintained and used, and not cancelled by a high stiffness introduced by retrofit.

For future application of such retrofit solution, further research should be conducted on durability and humidity influence on the existing building elements.

ACKNOWLEDGEMENT

The authors acknowledge the kind cooperation and support of FIBEX and ASAHI BOND companies.

The financial support of the Japan Society for Promotions of Science (JSPS) postdoctoral research grant no. PE 13092 is acknowledged.

The authors also acknowledge the financial support of the Romanian National Authority for Scientific Research and Innovation, CNCS – UEFISCDI, project number PN-II-RU-TE-2014-4-2169".

REFERENCES

[1] Zhe Qu, Andreea Dutu, Jiangrong Zhong, and Jingjiang Sun (2015) Seismic Damage to Masonry-Infilled Timber Houses in the 2013 M7.0 Lushan, China, Earthquake. Earthquake Spectra: August 2015, Vol. 31, No. 3, pp. 1859-1874.

[2] Dutu, A., Ferreira, J. G., and Goncalves, A. (2012a). "The behaviour of timber framed masonry panels in quasi-static cyclic testing." 9th Int. Conf. on Urban Earthquake Engineering/4th Asia Conf. on Earthquake Engineering, Tokyo Institute of Technology, Tokyo.

[3] Poletti, E., and Vasconcelos, G. (2014). "Seismic behaviour of traditional timber frame walls: Experimental results on unreinforced walls." Bull. Earthquake Eng., 13(3), 885–916.

[4] Ruggieri, N., and Zinno, R. (2013). "Behavior of the Borbone constructive system under cyclic loading." 1st Int. Conf. on Historic Earthquake-Resistant Timber Frames in the Mediterranean Area (Heart), Univ. of Calabria, Cosenza, Italy.

[5] Vieux-Champagne, F., Sieffert, Y., Grange, S., Polastri, A., Ceccoti, A., and Daudeville, L. (2014). "Experimental analysis of seismic resistance of timber-framed structures with stones and earth infill." Eng. Struct., 69, 102–115.

[6] Kouris L.A., Kappos A.J., (2014), "A practice-oriented model for pushover analysis of a class of timber-framed masonry buildings", Engineering Structures, Volume 75, 15 September 2014, Pages 489–506, doi:10.1016/j.engstruct.2014.06.012

[7] Dutu, A., Sakata, H., Yamazaki, Y., and Shindo, T. (2015). "In-Plane Behavior of Timber Frames with Masonry Infills under Static Cyclic Loading." J. Struct. Eng., 10.1061/(ASCE)ST.1943-541X.0001405, 04015140.

[8] Dutu, A., Sakata, H., Yamazaki, Y., and Shindo, T. (2015) Retrofit solution for timber framed masonry system using aramid fiber reinforced polymers (AFRP) - IABSE Symposium Report, 2015

[9] Oliveira, D.V., Basilio, I. and Lourenco P.B. 2011. Experimental Bond Behavior of FRP Sheets Glued on Brick Masonry, *Journal of Composites for Construction, ASCE, January/February*, 15:32-41

[10] Tezuka J., Noguchi T., Yamashita J., Hirabayashi Y., (2004) "Test report and experiment for making practicable timber structure joint reinforced with aramid fiber sheet" (In Japanese), *AIJ Annual meeting* 2004, p. 385